Application of Wavelets in Graphics

Lecture #5: Tuesday, Oct 14 1997
Lecturer: Eric Veach
Scribe: Li-Yi Wei
Reviewer: Li-Wei He

In this lecture we will talk about various applications of wavelets in graphics, with concentration on wavelet radiosity. Typical applications of wavelets in graphics and image processing include:

1. Image editing, compression, and retrieval [3, 4].
2. Curve and surface editing, compression, and variational modeling [2, 6].
3. Global illumination problems (e.g. radiosity) [7, 8, 9].

The book *Wavelets for Computer Graphics: Theory and Applications* by Stollnitz, DeRose, and Salesin [1] gives an overview of these applications.

1 Image Compression using Wavelets

One successful application of wavelets in image compression is finger print file compression [5]. The FBI has about 30 million finger print images, each with size about 10M bytes. Wavelet compression outperforms JPEG in compressing those finger print files. The main problem with JPEG is that it introduces blocking artifacts at high compression ratios, which can obscure the fingerprint "minutiae" (e.g. ridge endings).

Generally, image compression consists of the following steps:

1. Choose a basis. First we may want to divide the image into fixed sized blocks (e.g. as in JPEG). Then we choose a set of basis functions that has the desired properties, such as smoothness, vanishing moments, symmetry.
2. Transformation of the image, by projecting it into the chosen basis.
3. Quantization of the coefficients.
4. Coding. After quantization we could further compress the coefficients using lossy or lossless compression techniques.

The main reason for dividing the image into fixed sized blocks is to make the basis functions local. With wavelets this is not necessary since the basis functions already have local support.

Given a set of 1D scaling functions $\{\phi_{i,j}(x)\}$ and wavelets $\{\psi_{i,j}(x)\}$, there are two ways to construct a 2D basis: standard basis and non-standard basis.

1.1 Standard Basis

In this case, we first apply a wavelet transform to all the rows of the original image, then we apply a wavelet transform to all the columns of the resulting coefficients. Let

$$\begin{array}{ll} V_i = \mathrm{Span}\{\phi_{i,j}(x)\}, & W_i = \mathrm{Span}\{\psi_{i,j}(x)\}, \\ V_i' = \mathrm{Span}\{\phi_{i,j}(y)\}, & W_i' = \mathrm{Span}\{\psi_{i,j}(y)\} \end{array}$$

from previous lectures we know

$$\begin{aligned} V_n &= V_0 \oplus W_0 \oplus W_1 \cdots \oplus W_{n-1} \\ V_n' &= V_0' \oplus W_0' \oplus W_1' \cdots \oplus W_{n-1}' \end{aligned}$$

Assume that the initial image $I \in V_n \times V_n'$, we can expand $V_n \times V_n'$ to be

$$V_n \times V_n' = V_0 \times V_0' \quad \oplus \quad \sum_{j=0}^{n-1} V_0 \times W_j' \quad \oplus \quad \sum_{j=0}^{n-1} W_j \times V_0' \quad \oplus \quad \sum_{i=0}^{n-1}\sum_{j=0}^{n-1} W_i \times W_j'$$

In other words, we project the original image $I \in V_n \times V_n'$ into the following set of basis functions:

$$\begin{array}{ll} \phi_{00}(x)\phi_{00}(y) & \phi_{00}(x)\psi_{j'k'}(y) \\ \phi_{jk}(x)\psi_{00}(y) & \psi_{jk}(x)\psi_{j'k'}(y) \end{array}$$

where $j = 0 \ldots n-1$, $k = 0 \ldots 2^j - 1$, and similarly for j', k'.

The disadvantage of the above set of basis functions is that they have bad support shape. For example, for those $\phi_{00}(x)\psi_{j'k'}(y)$, they could be wide in the x dimension and narrow in the y dimension(they look like horizontal strips). Those basis functions won't represent the original image locally, so they are a bad set of basis functions.

1.2 Non-standard Basis

In contrast with standard basis function, non-standard basis transforms the original image $I_n \in V_n \times V_n'$ in an interleaved fashion. First we use one pass of wavelet transform to all the rows, then we do the same thing for all the columns. After one pass the image will look like this:

$$\left(\begin{array}{cc} \left(V_{n-1} \times V_{n-1}' \right) & \left(V_{n-1} \times W_{n-1}' \right) \\ \left(W_{n-1} \times V_{n-1}' \right) & \left(W_{n-1} \times W_{n-1}' \right) \end{array} \right)$$

We can repeat the above process to the upper-left subimage $I_{n-1} \in V_{n-1} \times V_{n-1}'$ and conitue in similar fashion until we have $I_0 \in V_0 \times V_0'$. The above operations could be written algebraically as:

$$\begin{aligned} V_n \times V_n' &= V_0 \times V_0' \quad \oplus \quad \sum_{i=1}^{n} (V_i \times V_i' - V_{i-1} \times V_{i-1}') \\ &= V_0 \times V_0' \quad \oplus \quad \sum_{i=1}^{n} (V_{i-1} \times W_{i-1}' \quad \oplus \quad V_{i-1}' \times W_{i-1} \quad \oplus \quad W_{i-1} \times W_{i-1}') \end{aligned}$$

In other words, we project the original image $I \in V_n \times V_n'$ into the following set of basis functions:

$$\begin{array}{cc} \phi_{00}(x)\phi_{00}(y) & \phi_{jk}(x)\psi_{jk'}(y) \\ \phi_{jk}(x)\psi_{jk'}(y) & \psi_{jk}(x)\psi_{jk'}(y) \end{array}$$

where $j = 0 \ldots n-1$ and $k, k' = 0 \ldots 2^j - 1$.

For non-standard basis, the filter supports are more localized than standard basis since all the products only involve scaling functions and wavelet functions of the same level. As you might expect the non-standard basis usually gives more compression ratio than the standard basis.

2 Wavelet Radiosity

The final section will talk about wavelet radiosity. For more information, please consult [8], [9] and [10].

The radiosity equation could be written as:

$$B(x) = E(x) + \int K(x,y)B(y)\,dy \tag{1}$$

where x and y are points on 2D scene surfaces.

Since the above equation is an integral equation, we have to project it into a finite basis to solve it. In traditional radiosity method, we first divide the environment into N surface patches, associate N basis functions with those patches, project the above equation into a matrix form, and use numerical algorithms like Jacobian iteration to solve the linear system. The problem is that it's very expensive to project the kernel $K(x, y)$ into a $N \times N$ matrix. In [7] they use hierarchical algorithm to reduce the computation time from $O(N^2)$ to $O(k^2 + N)$ using box basis functions, where k is the number of initial patches and N is the number of subdivided elements. [8] and [9] further extends the ideas by using wavelet basis functions. The merit is that by doing so we can get a better discretization of the kernel $K(x, y)$, thus throwing away those smaller coefficients does not hurt too much.

Let $V = \mathrm{Span}\{B_i(x), i = 1 \ldots N\}$ to be the function space spanned by basis $\{B_i(x)\}$. The approximate solution $\hat{B}(x)$ is represented as a linear combination of these basis functions:

$$\hat{B}(x) = \sum_{i=1}^{N} b_i B_i(x) \ .$$

Assume that $\{B_i(x)\}$ is orthonormal, and define operator P_v to be the projection of a function f to V, i.e.

$$P_v(f) = \sum_i \langle f, B_i \rangle B_i$$

Another way to think about this is that P_v transforms a function f into a column vector V_f which is of dimension N and contains the coefficients of the projection.

We now solve the approximate equation

$$\hat{B}(x) = (P_v E)(x) + (P_v K P_v \hat{B})(x)$$

where $\hat{K} = P_v K P_v$ is the approximate transport operator. Because of the leftmost P_v, $\hat{B}(x)$ lies in the subspace V and can be represented by its coefficients b_i.

Mathematically, let

$$\begin{aligned}
\hat{E}(x) &= \sum_{i=1}^{N} \langle E(x), B_i(x) \rangle B_i(x) \;=\; \sum_{i=1}^{N} e_i B_i(x) \\
\hat{K}(x,y) &= \sum_{i=1}^{N} \sum_{j=1}^{N} \langle \langle K(x,y), B_i(x) \rangle, B_j(y) \rangle B_i(x) B_j(y) \\
&= \sum_{i=1}^{N} \sum_{j=1}^{N} k_{ij} B_i(x) B_j(y)
\end{aligned}$$

Then

$$\begin{aligned}
\int \hat{K}(x,y) \hat{B}(y)\, dy &= \int (\sum_{i=1}^{N} \sum_{j=1}^{N} k_{ij} B_i(x) B_j(y)) (\sum_{k=1}^{N} b_k B_k(y))\, dy \\
&= \sum_{i=1}^{N} \sum_{j=1}^{N} \sum_{k=1}^{N} k_{ij} b_k B_i(x) \int B_j(y) B_k(y)\, dy \\
&= \sum_{i=1}^{N} \sum_{j=1}^{N} k_{ij} b_j B_i(x)
\end{aligned}$$

since $\{B_i\}$ is orthonormal.

If we put the above result into equation (1) we have

$$b_i = e_i + \sum_{j=1}^{N} k_{ij} b_j$$

or in matrix form

$$\hat{B} = \hat{E} + \hat{K} \hat{B}, \quad \text{where}$$

$$\hat{B} = \begin{pmatrix} b_1 \\ b_2 \\ \vdots \\ b_N \end{pmatrix} \quad \hat{E} = \begin{pmatrix} e_1 \\ e_2 \\ \vdots \\ e_N \end{pmatrix} \quad \hat{K} = \begin{pmatrix} k_{11} & k_{12} & \cdots & k_{1N} \\ k_{21} & k_{22} & \cdots & k_{2N} \\ \vdots & \vdots & \ddots & \vdots \\ k_{N1} & k_{N2} & \cdots & k_{NN} \end{pmatrix}$$

The above linear system is the discretized version of equation (1). We could solve it using other numerical algorithms and get an approximate solution for the projected radiosity function $\hat{B}$.

For wavelet radiosity, wavelets are used for the basis functions $B_i(x)$. Note that for 3D scene, the variables x and y are actually 2D surface points, so the kernel $K(x, y)$ is a 4D function. Thus we need to project the kernel onto basis functions that are a product of four 1D basis functions. This can be done in either the standard or non-standard ways as described above.

If we compare image compression using wavelets and wavelet radiosity we can find many similarities between them. The digital image is a discretized version of some continous image. In otherwords, we can think we project the original continous image into a set of basis functions and use the coefficients to represent the original image. In both image compression and wavelet radiosity, we try to find a good basis so that we can throw away many coefficients with sacrificing the quality.

The following compares the results of wavelet radiosity in flatland using different bases:

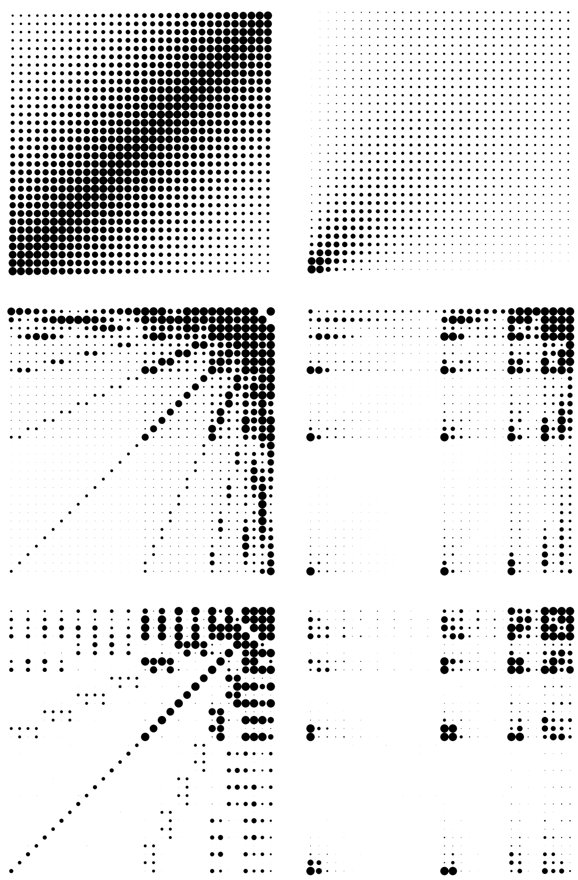

Figure 1: The left column shows the matrix of the flatland kernel for two parallel line segments in the finest level basis, the standard Haar basis and the standard F_2 basis(top to bottom). The right column shows the matrix of the flatland kernel for two line segments meeting at right angles in the same three bases.

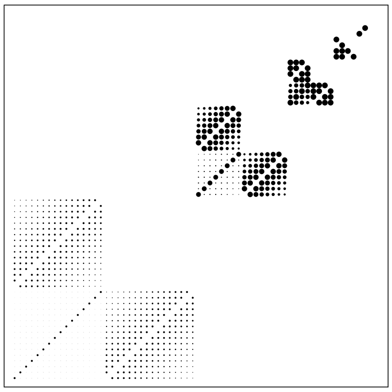

Figure 2: The kernel for two parallel lines realized in the non-standard Haar basis.

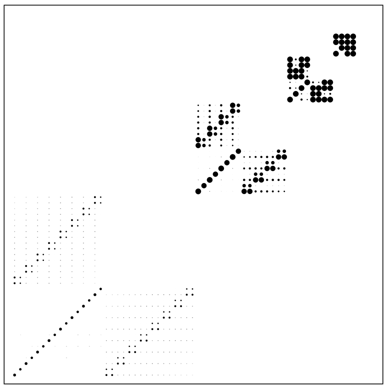

Figure 3: The kernel for two parallel lines realized in the non-standard F_2 basis.

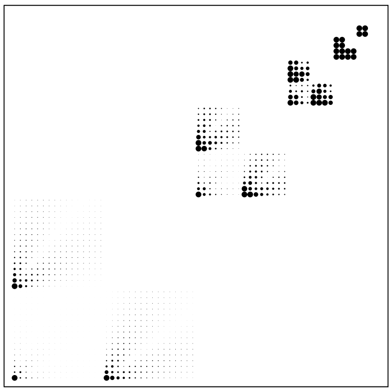

Figure 4: The kernel for two perpendicular lines realized in the non-standard Haar basis.

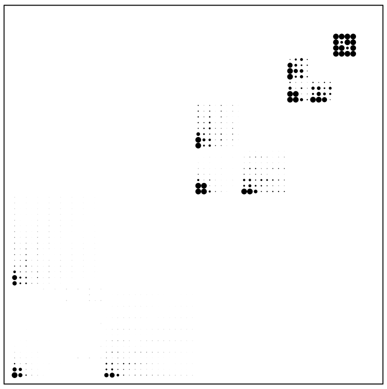

Figure 5: The kernel for two perpendicular lines realized in the non-standard F_2 basis.

Figure 1 compares Haar basis with F_2 basis for standard case. We can see F_2 gives better result since the resulting matrix contains more small elements. Figure 2, 3, 4, 5 show that for non-standard case, F_2 basis gives better result than Haar basis. Figure 6, 7 compares more different bases in wavelet radiosity.

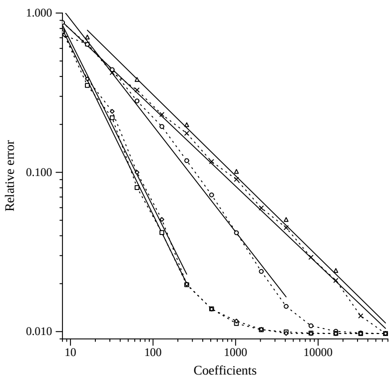

Figure 6: Parallel segments: Relative L^1 error plotted against number of coefficients used with full matrices, non-standard haar, standard haar, non-standard F_2, and standard F_2 bases (top to bottom).

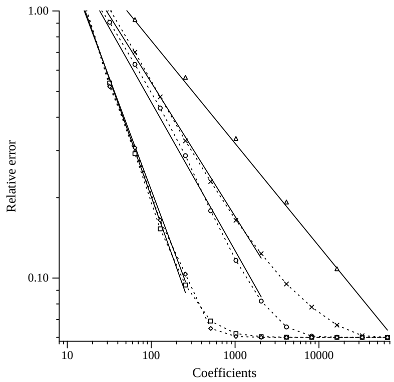

Figure 7: Perpendicular segments: Relative L^1 error plotted against number of coefficients used with full matrices, non-standard haar, standard haar, non-standard F_2, and standard F_2 bases (top to bottom).

References

[1] Eric J. Stollnitz, Tony D. DeRose, and David H. Salesin *Wavelets for Computer Graphics: Theory and Applications.* Morgan Kauffmann, San Francisco, 1996.

[2] Adam Finkelstein, David H. Salesin. *Multiresolution Curves.* In Proceedings of SIGGRAPH '94, pages 261-268. ACM, New York, 1994.

[3] Deborah F. Berman, Jason T. Bartell, David H. Salesin. *Multiresolution Painting and Compositing.* Proceedings of SIGGRAPH 94, in Computer Graphics Proceedings, Annual Conference Series, 85-90, July 1994.

[4] Charles E. Jacobs, Adam Finkelstein, David H. Salesin. *Fast Multiresolution Image Querying.* Proceedings of SIGGAPH 95, in Computer Graphics Proceedings, Annual Conference Series, pages 277-286, August 1995.

[5] *Fingerprints go digital.* Survey article directed towards mathematicians. In: Notices Amer. Math. Soc., v. 42 no. 11, pp. 1278-1283, Nov. 1995. (formerly AAAS95) Author: C. Brislawn.

[6] Gortler, S.J. et al. *Hierarchical and variational geometric modeling with wavelets* Proceedings 1995 Symposium on Interactive 3D Graphics. Held: Monterey, CA, USA 9-12 April 1995. Proceedings 1995 Symposium on Interactive 3D Graphics (1995) p. 35-42, 205 (Conference Paper)

[7] Hanrahan, P., Salaman, D., and Aupperle, L. *A Rapid Hierarchical Radiosity Algorithm. Computer Graphics 25, 4* (July 1991), 197-206

[8] Steven J. Gortler, Peter Schroder, Michael F. Cohen and Pat Hanrahan. *Wavelet Radiosity.* In *Computer Graphics, Annual Conference Series, 1003* (August 1993), Siggraph.

[9] Peter Schroder, Steven J. Gortler, Michael F. Cohen and Pat Hanrahan. *Wavelet Projections for Radiosity.*

[10] Michael F. Cohen and John R. Wallace. *Radiosity and Realistic Image Synthesis.* Academic Press Professional, 1993